Available online at www.sciencedirect.com
ScienceDirect
Thin Solid Films xx (2007) xxx–xxx
thin solid films
www.elsevier.com/locate/tsf

Optical and electrical properties of co-sputtered amorphous transparent conducting zinc indium tin oxide thin films

K.J. Saji, M.K. Jayaraj *

Optoelectronic Devices Laboratory, Department of Physics, Cochin University of Science and Technology, Kochi - 682 022, India

Received 6 June 2007; received in revised form 18 October 2007; accepted 19 October 2007

Abstract

Highly conductive and transparent thin films of amorphous zinc indium tin oxide are prepared at room temperature by co-sputtering of zinc oxide and indium tin oxide. Cationic contents in the films are varied by adjusting the power to the sputtering targets. Optical transmission study of films showed an average transmission greater than 85% across the visible region. Maximum conductivity of 6×10^{2} S cm^{-1} is obtained for Zn/In/Sn atomic ratio 0.4/0.4/0.2 in the film. Hall mobility strongly depends on carrier concentration and maximum mobility obtained is 18 cm^{2} V^{-1} s^{-1} at a carrier concentration of 2.1×10^{20} cm^{-3}. Optical band gap of films varied from 3.44 eV to 3 eV with the increase of zinc content in the film while the refractive index of the films at 600 nm is about 2.0.
© 2007 Published by Elsevier B.V.

Keywords: Amorphous oxides; Transparent conducting oxides; Co-sputtering; Zinc indium tin oxide

1. Introduction

Demands for transparent and conducting materials are rapidly growing in technical applications such as transparent electrode materials for liquid crystal displays, solar cells, smart windows etc. Several crystalline transparent conducting oxides (TCOs) in thin film form have been reported in literature. This include In_2O_3:Sn, ZnO:Al [1], $MgIn_2O_4$ [2], $ZnGa_2O_4$ [3], $Cd_{1-x}Y_xSb_2O_6$ [4], $AgSbO_3$ [5], and $InGaZnO_4$ [6]. Amorphous TCOs have recently been got much attraction owing to its applications in large area flexible displays, invisible electronic circuits and amorphous solar cells. Electrically conducting and visibly transparent amorphous materials have unique advantage of low temperature processing over crystalline materials. This enables the deposition of thin films of these amorphous materials on plastic substrates. Several amorphous TCOs such as indium oxide [7,8], indium gallium zinc oxide [9], cadmium germinate [10,11], zinc tin oxide and zinc indium oxide and its use in electronic circuits have been reported [12–16]. These materials exhibit excellent optical transmission, high electrical conductivity and high chemical stability [17–20].

Detailed description of working hypothesis of amorphous TCOs was given by Hosono et al. [21]. Amorphous metal oxides composed of heavy metal cations with an electronic configuration $(n-1)d^{10}ns^{0}$ with $n\geq4$ shows a large overlap between conduction band orbitals. The magnitude of these overlap are insensitive to the structural randomness which is intrinsic to the amorphous state since the bottom part of the conduction band is primarily composed of the spherically symmetric *ns* orbital of heavy metal.

In this paper we describe the preparation and characterization of an amorphous TCO, zinc indium tin oxide (ZITO) prepared by the co-sputtering of zinc oxide and indium tin oxide. Room temperature deposited films have excellent electrical conductivity without annealing or ion implantation. Negative sign of Hall coefficient was observed, showing that carriers responsible for conduction are electrons.

2. Experimental details

ZITO thin film samples were prepared by the co-sputtering method using powders of ZnO (99.99% pure) and $In_{0.5}Sn_{0.5}O_2$ (ITO) (99.99% pure). Schematic diagram of the deposition technique is given in Fig. 1. ZnO target was powered by a radio

* Corresponding author. Tel.: +91 484 2577404; fax: +91 484 2577595.
E-mail address: mkj@cusat.ac.in (M.K. Jayaraj).

0040-6090/$ - see front matter © 2007 Published by Elsevier B.V.
doi:10.1016/j.tsf.2007.10.097

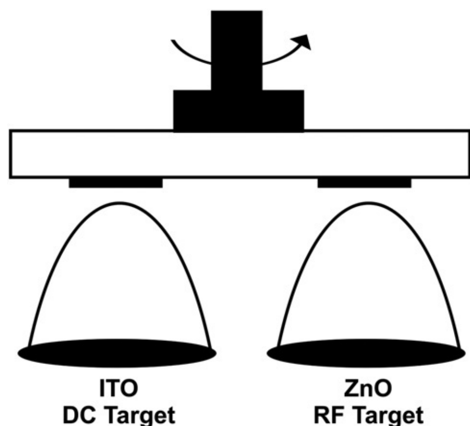

Fig. 1. Schematic diagram of the co-sputtering setup used for the growth of ZITO films.

frequency (RF) power source and ITO target by a direct current (DC) power source. DC target (ITO) current was fixed at 200 mA (600 V) and power to RF target (ZnO) was varied from 25 W to 200 W in 25 W steps. Sputtering was carried out for 10 min in pure argon atmosphere. Glass substrates were placed parallel to the targets at a distance of 4 cm from target surfaces and were not intentionally heated during the deposition. Substrate was rotated over the targets at a speed of 50 rotations per minute using a stepper motor assembly. Composition of deposited films can be easily controlled by adjusting the power to sputtering targets.

The film structures were characterized by glancing angle X-ray diffraction (XRD) at an incident angle of 0.5° using RIGAKU RINT-2000 with Cu Kα radiation. Film surface morphologies were analysed by atomic force microscopy (AFM, using SPI — 3800N, S.I.I.). Film thickness was measured by Veeco Dektak 6M stylus profiler. Optical absorption spectra were recorded using a UV–VIS–NIR spectrophotometer (Hitachi U — 4000). The resistivity, carrier concentration and Hall mobility were obtained by Hall effect measurements using a four probe van der Pauw configuration. Chemical composition of the films was analyzed by X-ray fluorescence (XRF, model ZSX100E, Rigaku) spectroscopy.

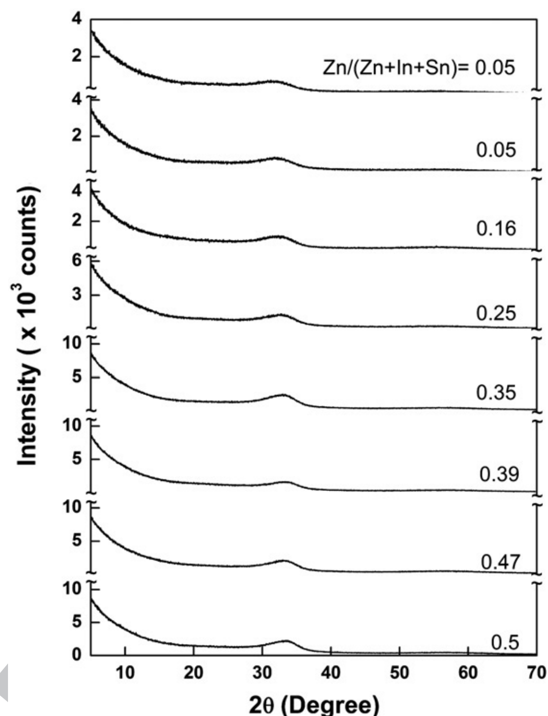

Fig. 3. Glancing angle X-ray diffraction pattern of ZITO films for various Zn content showing the amorphous nature.

3. Results and discussion

Fig. 2 shows the deposition rate of films with respect to the variations of RF power. Thickness varies from 295 nm for films deposited at 25 W to 430 nm for films deposited at 200 W for a deposition time of 10 min. Glancing angle XRD profiles of as deposited films shown in Fig. 3 have only a halo peak around 34° and there are no sharp peaks. This indicates that all films are

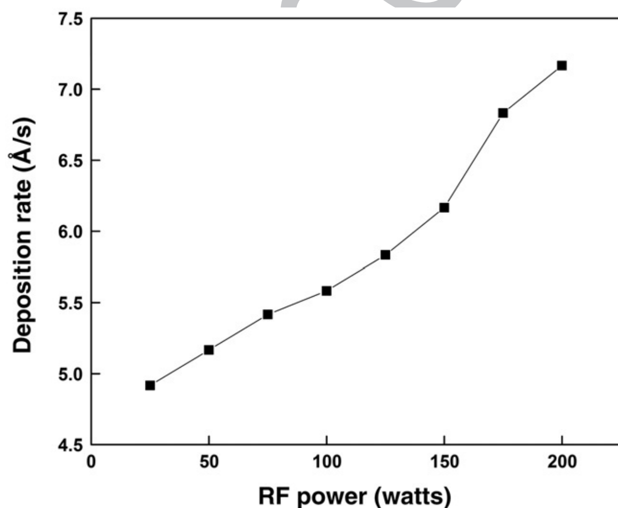

Fig. 2. The deposition rate of ZITO films for various RF power to the ZnO target keeping a constant DC current of 200 mA for ITO target.

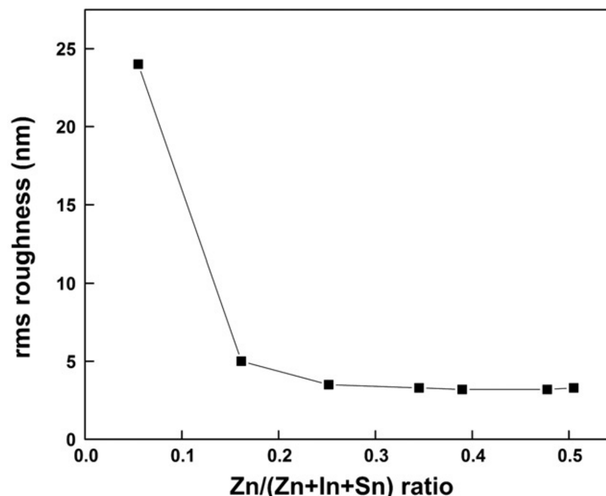

Fig. 4. Variation of rms roughness of the films with different Zn content.

ARTICLE IN PRESS

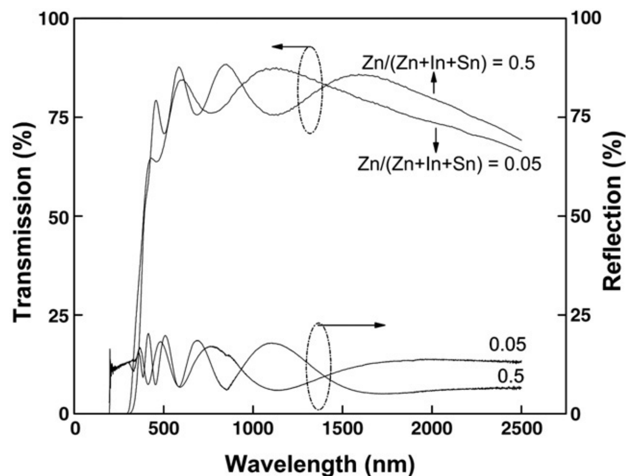

Fig. 5. Optical transmission and reflection spectra of co-sputtered amorphous ZITO films.

amorphous irrespective of variations in RF power and composition. Presence of zinc, indium and tin in the co-sputtered films was confirmed by XRF analysis. The Zn/In/Sn atomic ratios varied from 0.05/0.56/0.39 to 0.5/0.27/0.23 in the co-sputtered films by varying the RF power. Film roughness was estimated from AFM analysis and found an rms roughness of approximately 3 nm except for the film with low Zn content (Fig. 4).

Optical transmission spectra show an average transmission greater than 85% for all films in the visible region of electromagnetic spectrum (Fig. 5). An abrupt decrease in transmission at lower wavelength is due to fundamental band to band absorption and loss of transmission at higher wavelength is attributed to the absorption by carrier electrons. In amorphous semiconductors, the valence and conduction bands have tails of localized states, and the energy that separates the localized states from the delocalized state is called the mobility edge. A sharp drop in the mobility by a factor of about 10^2 has been generally observed at the mobility edge in amorphous materials [22]. High carrier densities and mobilities (discussed later) in co-sputtered ZITO films indicate that the Fermi level in these amorphous films exceeds the mobility edge of the conduction band.

The refractive index of the films was estimated from the optical transmission data by the method described by Swanepoel [23]. We got an average refractive index of 2.0 at 600 nm for amorphous ZITO films. These values remained almost steady with the variation of zinc content in the film (Fig. 6).

The absorption coefficient α of semiconductors generally follows a relationship of the form

$$\alpha h\nu = (\mathrm{const})\left(\mathrm{h}\nu - E_g^{\mathrm{opt}}\right)^r. \quad (1)$$

Optical band gap E_g^{opt} is then obtained by linearly extrapolating the plot of $(\alpha \mathrm{h}\nu)^{1/r}$ vs. hν and finding the intersection

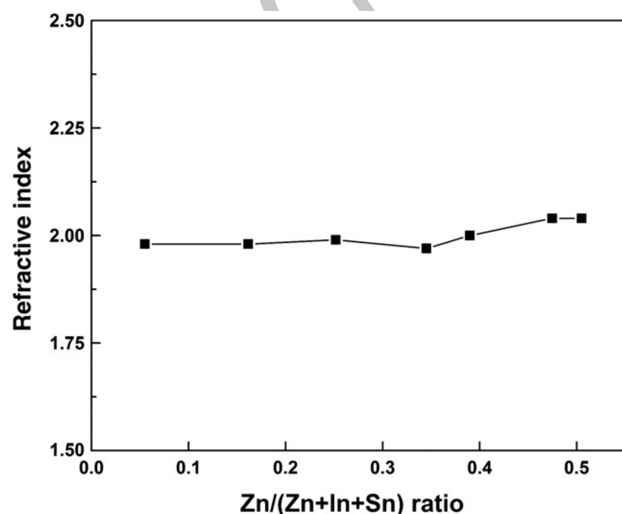

Fig. 6. Refractive index of amorphous ZITO films at 600 nm.

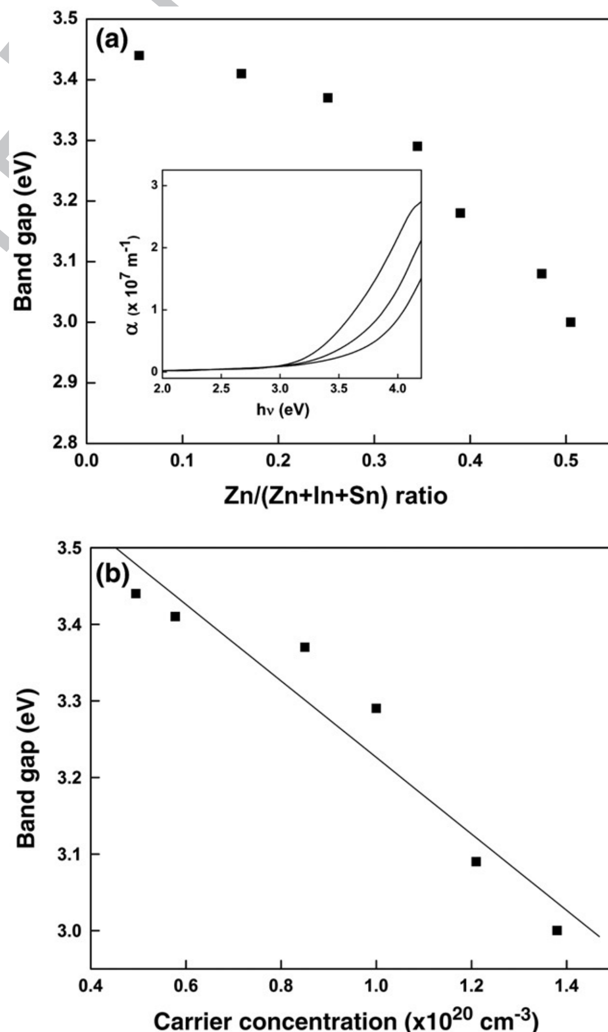

Fig. 7. (a) Band gap variation with the variation of zinc content in the film. Inset shows the plot of absorption coefficient (α) for different zinc concentration (lower line Zn/(Zn + In + Sn) = 0.05, middle line Zn/(Zn + In + Sn) = 0.35 and top line Zn/(Zn + In + Sn) = 0.5) (b) Dependence of band gap on carrier concentration of the film.

UNCORRECTED PROOF

Please cite this article as: K.J. Saji, M.K. Jayaraj, Thin Solid Films (2007), doi:10.1016/j.tsf.2007.10.097

ARTICLE IN PRESS

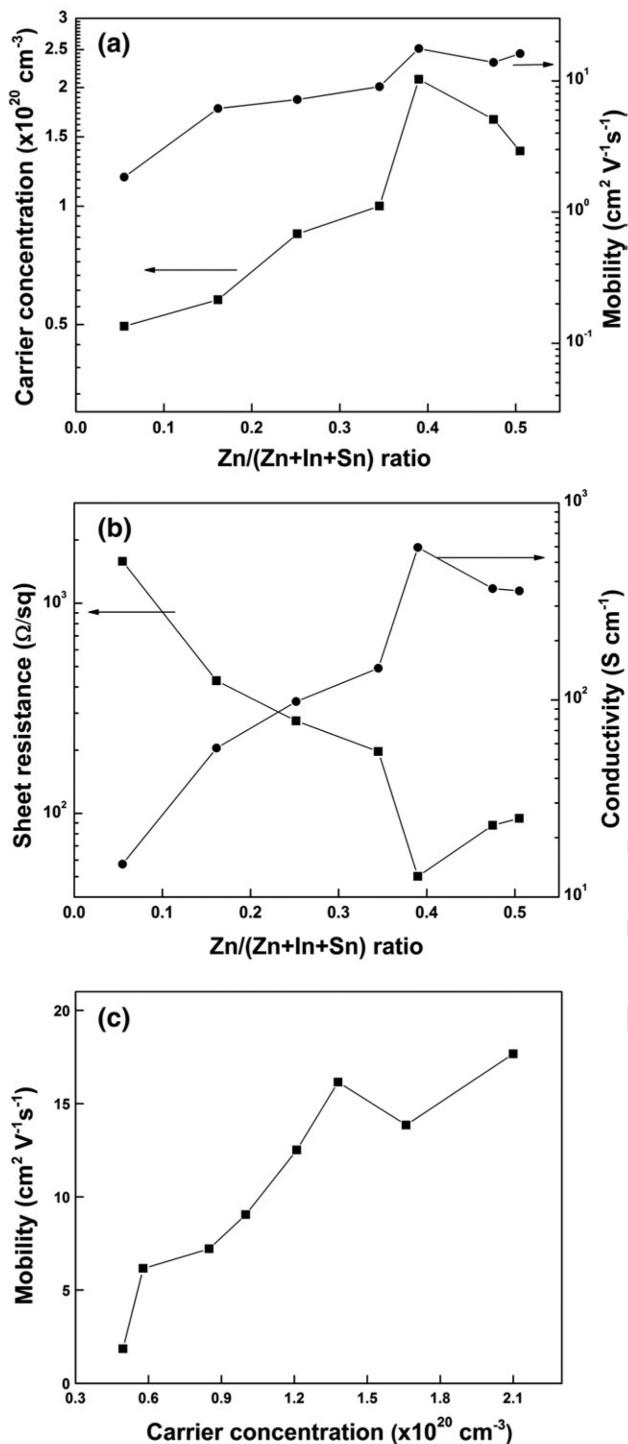

Fig. 8. (a) Variation of Hall mobility and carrier concentration with the increase of zinc content in amorphous ZITO films. (b) Sheet resistance and conductivity variation with zinc content. (c) Dependence of Hall mobility on carrier concentrations.

with the abscissa. Tauc et al. showed that $r=2$ holds in amorphous semiconductors assuming parabolic bands [24].

Optical band gap of the films were found by plotting $(\alpha h\nu)^{0.5}$ vs. hν and extrapolating to the energy axis. Band gap thus obtained varied from 3.44 eV to 3 eV with the increase of zinc content in the film. Fig. 7 shows the variations of optical band gap of co-sputtered ZITO films with the increase of zinc content. It shows that the band gap of the films can be easily tuned by just varying the power (and hence the composition of the films) to the sputtering targets. Insect shows a plot of absorption coefficient of films. Since the band gap of ZnO is less than that of ITO, an increase in zinc content causes the decrease of ZITO band gap. At the same time, carrier densities of ZITO films get enhanced by the increase of zinc content. This causes the band gap to decrease with the increase of carrier density in the film (Fig. 7b).

Conductivity, carrier concentration and hall mobility of the co-sputtered ZITO films are shown in Fig. 8. Mobility and carrier concentration increases with Zn content in the film. Hence conductivity shows an increasing tendency with the increase of Zn content. Maximum conductivity of 6×10^2 S cm^{-1} is obtained for Zn/In/Sn atomic ratio 0.4/0.4/0.2 in the film. Hall mobility strongly depends on carrier concentration and steeply increases from ~2 cm^2 V^{-1} s^{-1} to 12.5 cm^2 V^{-1} s^{-1} as the carrier concentration slightly increases from 4×10^{19} cm^{-3} to 1.2×10^{20} cm^{-3}. Maximum mobility obtained is 18 cm^2 V^{-1} s^{-1} at a carrier concentration of 2.1×10^{20} cm^{-3}. The mean free path length l is calculated using the equation

$$l=\frac{(3\pi^2)^{1/3}hn^{1/3}\mu}{2\pi e}, \quad (2)$$

where h, n, e and μ denote the Planck constant, carrier density, elementary electric charge and mobility respectively. Estimated mean free path length varies from 1.4 Å to 2 nm as the carrier concentration varies from 5×10^{19} cm^{-3} to 2.1×10^{20} cm^{-3}.

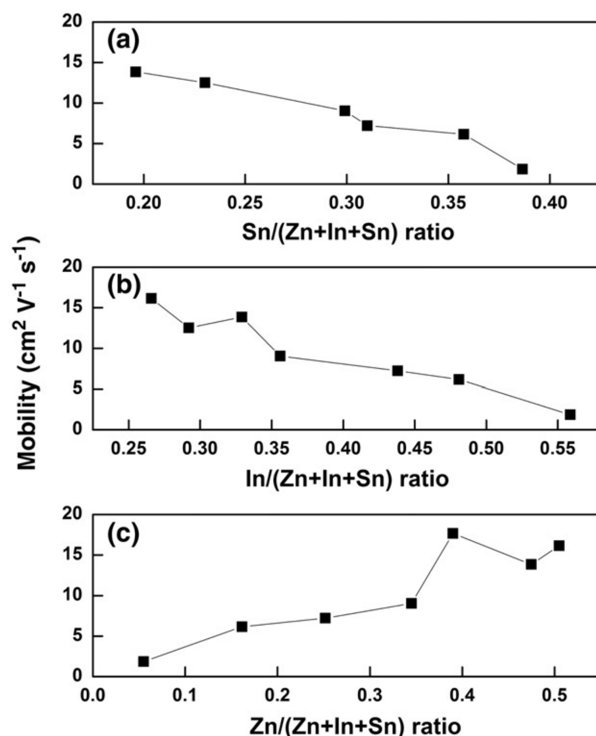

Fig. 9. Hall mobility variation with (a) tin (b) indium and (c) zinc cationic contents in amorphous ZITO films.

Please cite this article as: K.J. Saji, M.K. Jayaraj, Thin Solid Films (2007), doi:10.1016/j.tsf.2007.10.097

ARTICLE IN PRESS

Variation of Hall mobility with respect to the increase of different cationic content in the film is shown in Fig. 9. As tin and indium content increases, the mobility shows a gradual decrease, while it increases with the increase of zinc content.

Observed characteristics of amorphous ZITO films can be explained on the basis of working hypothesis of wide band gap electrically conducting amorphous oxides [20]. Inverse photoelectron spectroscopic and molecular orbital studies carried out on similar amorphous TCOs shows that the density of states of conduction band bottom of these amorphous materials are almost same as in the crystalline material [9,25]. Even though the topological sequence of the ion arrangement in heavy metal-oxide systems is metal-oxygen-metal, the conduction band bottom is primarily composed of vacant s orbitals of the heavy metal cations and the contribution of the intervening oxygen is rather small.

For complex amorphous systems containing several metal ions, the percolation theory should be taken into consideration [25]. The site percolation threshold decreases as the site density increases, and reaches the value of 0.20 for close packed fcc systems [26]. Hence the metal ions that play the dominant role in providing conductivity should occupy more than 20% of all ion sites in an amorphous phase. In our case the Zn (which forms conduction band bottom) content varies from 5% to 50% of total cation content. The carrier transport in a-ZITO may be governed by percolation conduction over the distribution of potential barriers around the conduction band edge. Non-localized tail states may form in the vicinity of conduction band bottom with potential barriers due to the random distribution of Zn^{2+}, In^{3+}, Sn^{2+}, and Sn^{4+} ions in amorphous structures. As carrier concentration increases the potential barriers are overcome, and therefore the Hall mobility increases with the increase of carrier concentration, and large Hall mobilities ($>15\ cm^2\ V^{-1}\ s^{-1}$) are obtained at carrier concentrations $\sim 10^{20}\ cm^{-3}$.

Even though the long range order is lost in present amorphous films, the Sn 5s, In 5s and/or Zn 4 s orbitals can form conduction path, since the content of these ions are greater than the percolation threshold of 20%. The condition for the formation of conduction path in amorphous oxides has been explained by Orita et al. by the evaluation of an overlap integral S, between ns orbital functions of various metal ions [9]. This overlap integral strongly depends on the principal quantum number n and the core charge Z. They suggest a threshold value of 0.4 for overlap integral as a criterion for the formation of extended wave functions which are responsible for the good conductivity. The overlap integrals between ns wave functions for Zn 4s, In 5s and Sn 5s orbitals are 0.6045, 0.5613, and 0.4523 respectively [9]. These values, originally derived for crystalline metal oxides, are also applicable to the amorphous phase since the overlap integrals of s orbitals simply depends on the metal–metal distance for a fixed metal ion. In our observation, the Hall mobility is found to increase with the increase of Zn content in the film. As the zinc content increases, the Zn–Zn average distance becomes shorter, and direct overlap between 4s orbitals of neighboring zinc cations is possible in the films. On the other hand, the Hall mobility decreases with the increase of In and Sn content. This observation, along with the fact that In 5s and Sn 5s orbitals have a low overlap integral value compared to Zn 4s orbitals, suggests that the conduction path in amorphous ZITO films are primarily formed by 4s orbital of Zn^{2+} ions.

4. Conclusion

Conductive and transparent thin films of amorphous zinc indium tin oxide are prepared at room temperature by co-sputtering of zinc oxide and indium tin oxide. Film compositions are varied by adjusting the power to the sputtering targets. Hall mobility is found to strongly depend on the type of cationic contents in the films. The conduction band bottom, controlling electron transport properties in amorphous ZITO films, are primarily composed of Zn 4s orbital and the magnitude of overlap between neighboring orbitals is large and insensitive to the structural randomness. The electronic structure is dominated by local atomic structures, which in amorphous oxides is close to the situation in a crystal. Hence the electron mobility of these materials is comparable with that in the crystalline state. This behaviour is in contrast with the low mobility situation in tetrahedral amorphous semiconductors like hydrogenated amorphous silicon (a-Si:H) where the electron conduction paths are composed of s–p hybrid orbitals and carrier transport is controlled by nearest neighbor hopping or variable range hopping.

Acknowledgments

One of the author (KJS) thanks the Centre of Excellence in Lasers and Optoelectronic Sciences for research fellowship. The authors thank Prof. Kamiya and Prof. Hosono of Tokyo Institute of Technology for the permission to use the XRF and Hall measurements. The authors also thank Kerala State Council for Science, Technology and Environment for the support under SARD program.

References

[1] K.L. Chopra, S. Major, D.K. Pandra, Thin Solid Films 102 (1983) 1.
[2] N. Ueda, T. Omata, N. Hikuma, K. Ueda, H. Mizoguchi, T. Hashimoto, H. Kawazoe, Appl. Phys. Lett. 61 (1992) 1054.
[3] T. Omata, N. Ueda, K. Ueda, H. Kawazoe, Appl. Phys. Lett. 64 (1994) 1077.
[4] K. Yanagawa, Y. Ohki, T. Omata, H. Hosono, N. Ueda, H. Kawazoe, Appl. Phys. Lett. 65 (1994) 406.
[5] M. Yasukawa, H. Hosono, N. Ueda, H. Kawazoe, J. Ceram. Soc. Jpn., Int. Ed. 103 (1995) 455.
[6] M. Orita, H. Tanji, M. Mizuno, H. Adachi, I. Tanaka, Phys. Rev., B 61 (2001) 1811.
[7] J.R. Bellingham, W.A. Phillips, C.J. Adkins, J. Phys., Condens. Matter 2 (1990) 6207.
[8] H. Nakazawa, Y. Ito, E. Matsumoto, K. Adachi, N. Aoki, Y. Ochiai, J. Appl. Phys. 100 (2006) 093706.
[9] M. Orita, H. Ohta, M. Hirano, S. Narushima, H. Hosono, Philos. Mag., B 81 (2001) 501.
[10] S. Narushima, H. Hosono, J. Jisun, T. Yoko, K. Shimakawa, J. Non-Cryst. Solids 274 (2000) 313.
[11] N. Kikuchi, H. Hosono, H. Kawazoe, K. Oyoshi, S. Hishita, J. Am. Ceram. Soc. 80 (1997) 22.

UNCORRECTED PROOF

Please cite this article as: K.J. Saji, M.K. Jayaraj, Thin Solid Films (2007), doi:10.1016/j.tsf.2007.10.097

ARTICLE IN PRESS

[12] K. Nomura, H. Ohta, A. Takagi, T. Kamiya, M. Hirano, H. Hosono, Nature 435 (2004) 488.
[13] H.Q. Chiang, J.F. Wager, R.L. Hoffman, J. Jeong, D.A. Keszler, Appl. Phys. Lett. 86 (2005) 013503.
[14] S. Kobayashi, S. Nonomura, T. Ohmori, K. Abe, S. Hirata, T. Uno, T. Gotoh, S. Nitta, S. Kobayashi, Appl. Surf. Sci. 113/114 (1997) 480.
[15] N.L. Dehuff, E.S. Kettenring, D. Hong, H.Q. Chiang, J.F. Wager, R.L. Hoffman, C.H. Park, D.A. Kezler, J. Appl. Phys. 91 (2005) 064505.
[16] M.S. Grover, P.A. Hersh, H.Q. Chiang, E.S. Kettenring, J.F. Wager, D.A. Keszler, J. Phys., D 40 (2007) 1335.
[17] T. Minami, H. Sonohara, T. Kakumu, S. Takata, Jpn. J. Appl. Phys. 34 (1995) L971.
[18] Y.S. Jung, Y.J. Seo, D.W. Lee, D.Y. Jeon, Thin Solid Films 445 (2003) 63.
[19] J.M. Phillips, R.J. Cava, G.A. Thomas, S.A. Carter, J. Kwo, T. Siegrist, J.J. Krajewski, J.H. Marshall, W.F. Peck Jr., D.H. Rapkine, Appl. Phys. Lett. 67 (1995) 2246.
[20] T. Sasabayashi, N. Ito, E. Nishimura, M. Kon, P.K. Song, K. Utsumi, A. Kaijo, Y. Shigesato, Thin Solid Films 445 (2003) 219.
[21] H. Hosono, N. Kikuchi, N. Ueda, H. Kawazoe, J. Non-Cryst. Solids 198–200 (1996) 165.
[22] E.A. Davis, N.F. Mott, Philos. Mag. 22 (1970) 903.
[23] R. Swanepoel, J. Phys., E J Sci. Instrum. 16 (1983) 1214.
[24] J. Tauc, R. Grigorovici, A. Vancu, Phys. Status Solidi, B Basic Res. 15 (1966) 627.
[25] S. Narushima, M. Orita, M. Hirano, H. Hosono, Phys. Rev., B 66 (2002) 035203.
[26] D. Stauffer, A. Aharony, Introduction to Percolation Theory, 2nd EditionTaylor & Francis, London, 1992.

UNCORRECTED PROOF

Please cite this article as: K.J. Saji, M.K. Jayaraj, Thin Solid Films (2007), doi:10.1016/j.tsf.2007.10.097